Comparison between physical and machine learning modeling to predict fretting wear volume

Soha Baydoun, Mohammed Fartas, Siegfried Fouvry

Comparison between physical and machine learning modeling to predict fretting wear volume

Soha Baydoun*, Mohammed Fartas, Siegfried Fouvry

Ecole Centrale de Lyon, LTDS Laboratory, 36 av Guy de Collongue, 69130 Ecully, France

*Corresponding authors email addresses: soha.baydoun@ec-lyon.fr (S. Baydoun)

Abstract

The objective of this study is to compare the performance of machine-learning strategy versus a physical friction-energy wear approach to predict the fretting wear volume of a low-alloyed steel contact by varying several loading parameters. Then, an artificial neural network (ANN) is used to predict the wear volume at each loading condition. These predictions were compared versus a physics-based friction energy wear modeling considering the third-body theory and the contact-oxygenation concept. A parametric study is performed to compare the prediction errors as a function of the proportion of the experiments involved in the modeling process. The results suggest that the physical modeling is more performant than ANN when a restricted number of experimental data is available for the calibration process.

Keywords: Fretting wear; Artificial Neural Network; Friction energy approach

1. Introduction

Fretting is a surface degradation process observed between two surfaces in contact submitted to normal load and undergoing small displacement oscillatory movements [1]. It has a profound impact on many engineering areas (nuclear applications, aeronautics, electrical contacts, cables, etc.) as it causes detrimental consequences reducing the durability of mechanical components. Depending on the applied displacement amplitude,

fretting can induce either cracking or wear damage if small or large sliding amplitudes are applied respectively [2,3]. Fretting wear activated under gross slip condition is considered a plague for contact assemblies as it leads to severe wear mechanisms as abrasion, adhesion, corrosion, seizure, etc. triggering ejection of wear particles [4]. It is well established that fretting is ruled by at least fifty parameters ranging from mechanical loading conditions, material properties, to surrounding environment [5–11]. The interactions between all these parameters render wear kinetics prediction a complex target if physics-based models are used.

Machine learning is a promising tool in forecasting the outcomes of complicated systems at elevated accuracy. Since its birth in the 20^{th} century, its usage has increased exponentially touching nearly all fields of modern science and engineering as medicine, computer vision, speech recognition, etc. Machine learning is a branch of artificial intelligence gathering statistical and optimization algorithms aiming at predicting the outcomes without being explicitly programmed to do so [12]. Artificial neural network (ANN) is a particular family of machine learning computing algorithms mimicking the performance of human neuron cells [13]. ANNs learn from data by trial and errors similar to the way biological cells learn from the outer environment. ANN was applied in tribology by Jones and co-authors in 1997 [13] who displayed the feasibility of the latter in predicting material wear response. Then, Velten and co-workers [14] extended this work by increasing the number of input variables and test conditions as well as the optimizing the prediction of the ANN. In fretting, several attempts were made to model the impact of loading conditions on fatigue and wear response [15–18]. For instance, fretting fatigue life duration as well as fretting crack lengths and stress intensity factor

were recently modeled by Nowell [19] and Gorji et al. [12] respectively revealing an interesting potential of ANN in such application. However, fretting wear volume and coefficient of friction were modeled by Velten et al. [14], Haviez et al. [17], and Kolodziejczyk and co-authors [20] revealing precise predictions of fretting wear response of materials at different experimental conditions. This latter work will be particularly extended in this article where a relatively bigger data base as well as higher number of inputs will be examined. For instance, in the current study, six fretting input parameters will be examined as the number of sliding cycles, the contact pressure, the sliding amplitude, the sliding frequency and finally the contact lengths parallel and perpendicular to the sliding direction. On the other hand, four input parameters are tested in [20] being the number of fretting cycles, the contact pressure, the displacement amplitude, and the surface roughness. Following this, the ANN wear volume predictions will be compared versus physics-based energy wear models taking into account the third body theory and the contact oxygenation concept. A parametric study will be then performed to compare the prediction errors as a function of the proportion of the experiments involved in the modeling process of each method.

2. Fretting wear experimental results

The experimental data in the current study (i.e. the wear volume at each loading condition) are extracted from previous publications [21,22] where the experimental work is carried out using the same test bench under the same environment by varying six loading parameters which will be detailed in the following sections. Only a few elements of the experimental approach are recalled here to better understand the experimental data considered.

2.1 Contact configuration and experimental setup

The investigated contact geometry was formed of a homogenous 34NiCrMo16 flat-on-flat configuration (Fig. 1a) characterized by a rectangular contact area "$A = L_C \times L_T$" where "L_C" is the longitudinal contact length collinear with the sliding direction (δ) and "L_T" is the transverse contact length perpendicular to the sliding direction (δ). A grinding process is applied on the flat specimens, which leads to a surface roughness Ra=0.25 µm. Tests were performed at ambient temperature (25 °C ± 5 °C) and relative humidity (RH=40% ± 10%) using a hydraulic test machine (Fig. 1b) customized specifically for testing large flat contacts (see Refs. [21,22]). This machine allows measuring the normal force and the sliding amplitude imposed during the test and recording the obtained tangential force and the coefficient of friction. It was shown that by varying several loading parameters, the friction coefficient was stable in this study at an average value equal to 0.7±0.04 as detailed in Refs. [21,22].

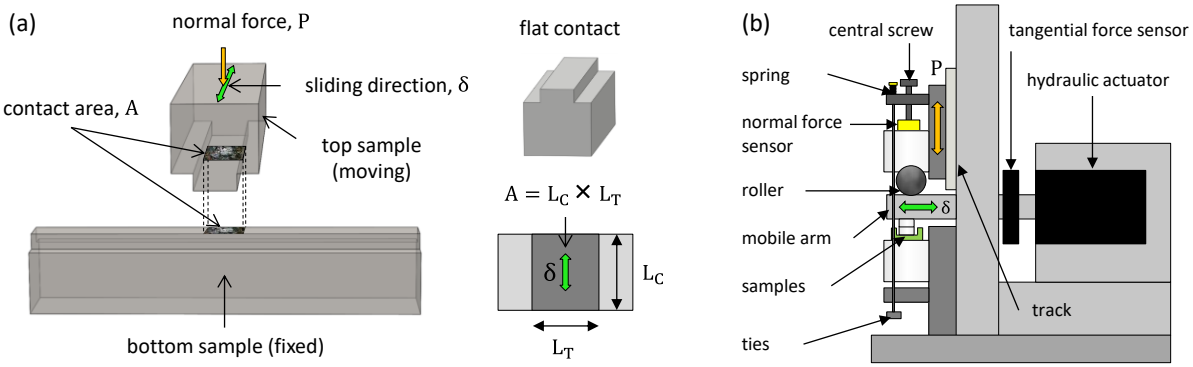

Fig. 1. Schematic illustration of the: (a) crossed flat-on-flat contact configuration and the (b) fretting wear experimental set-up.

2.2 Experimental strategy

A multi-scale test strategy was used starting from a reference key test condition (repeated three times) defined by a number of fretting cycles N=20000 cycles, contact pressure p=100 MPa, sliding amplitude δ_s= ±100 µm, sliding frequency f=1 Hz, and a square contact area A=25 mm² (L_C=L_T=5 mm) (Fig. 2). Then, a cross-experimental approach was used where each time one parameter was varied while fixing the others at the reference conditions. In this approach, the sliding amplitude was varied from δ_s= ±25 to ±200 µm (Fig. 2a), the contact pressure from p=25 to 175 MPa (Fig. 2a), the sliding frequency from f=0.5 to 10 Hz (Fig. 2b), the number of fretting cycles from N=5000 to 40000 cycles (Fig. 2b), and finally the contact area from A=2.5 to 25 mm² (Fig. 2c) by varying the contact lengths L_C and L_T separately as shown in Fig. 2c. Note that for contact lengths smaller than 2 mm, textured flat-on-flat samples were used instead of mono-contact configuration as fully detailed in Ref [22].

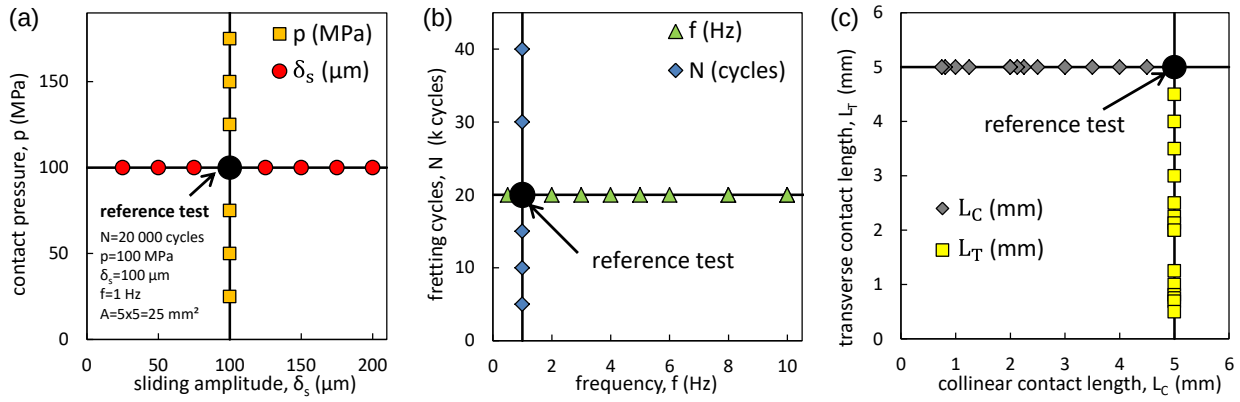

Fig. 2. Multi-scale experimental strategy proposed to study and model the influence of loading parameters on fretting wear damage: (a) contact pressure versus sliding amplitude; (b) number of fretting cycles versus sliding frequency; and (c) collinear contact length (L_C) versus transverse contact length (L_T) to the sliding direction.

To enrich the database with more complex loading conditions for validating and testing machine learning predictions, additional experiments were conducted such that two or more loading conditions are varied instead of one with respect to the reference test conditions (X_{ref}, Y_{ref}) with X and Y ∈ [N, p, δ_s, f, L_C, L_T]. By combining all the test conditions, a total of 150 tests is used for both training and validation of the neural network which are fully described in previous articles [21,23,24](Fig. 3).

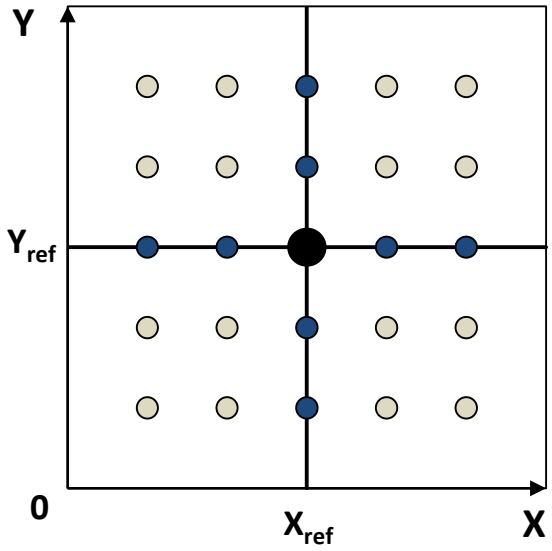

Fig. 3. Illustration of the additional tests used to enhance machine learning predictions such that (X_{ref}, Y_{ref}) are the reference loading conditions and X and Y∈ [N, p, δ_s, f, L_C, L_T].

3. Predicting wear volume using artificial neural network (ANN)

3.1 Neural network architecture

The ANN in this study is created using Matlab, in which a feed-forward artificial neural network is used. This latter consists of an input layer of six neurons where the loading conditions are introduced (Fig. 4) and one output layer where the wear volume is to be predicted. In between, three hidden layers are introduced with five neurons for the first layer, four neurons for the second and one neuron for the last hidden layer. The input,

hidden and the output layers are connected to each other by weights and biases. These latter are the core of the learning process which is accomplished by optimizing the weights and biases in order to reduce the error known as the loss function between the parameter to be predicted (i.e. experimental wear volume) and the output ANN predicted wear volume. These weights and biases are initialized with random values, then the optimization is fulfilled using backpropagation algorithm where the weights and biases are adjusted to reduce the loss function. The training backpropagation algorithm is Levenberg–Marquardt which uses interpolation between gradient-based and Gauss–Newton methods through iterative algorithm. The weights' adjustment is done each iteration known as "epoch" such that the learning process is run at several epochs until the weights are optimized. The speed for the learning procedure is adjusted using a hyper parameter known as the learning rate which is a parameter selected by the user to optimize the performance and the speed of the learning process.

For the first two hidden layers, the neuron activation functions used are sigmoidal tangent (tansig) and for the last hidden layer a linear purlin function is introduced. Analogous to the action potential rate firing in the brain, the activation function in each hidden neuron transforms the weighted input sum stemming from the previous neurons connected to it and outputs a value which allows deciding whether the neuron should be activated or not i.e. whether the neuron's input is important or not in the prediction process.

In order to train the neural network the input data must be split into three parts which are the training the data where the weights are optimized, validation data to check the performance of the network while training and finally the test data which correspond to

the set of data the model has never seen serving to check the performance of model and its generalization capacity. To obtain performant ANN, large quantity of data should be used and big portion of this data should be used for training. In this study, the data set (i.e. 150 experiments) will be split into 70% for training, 10% for validation and 20% for testing procedure.

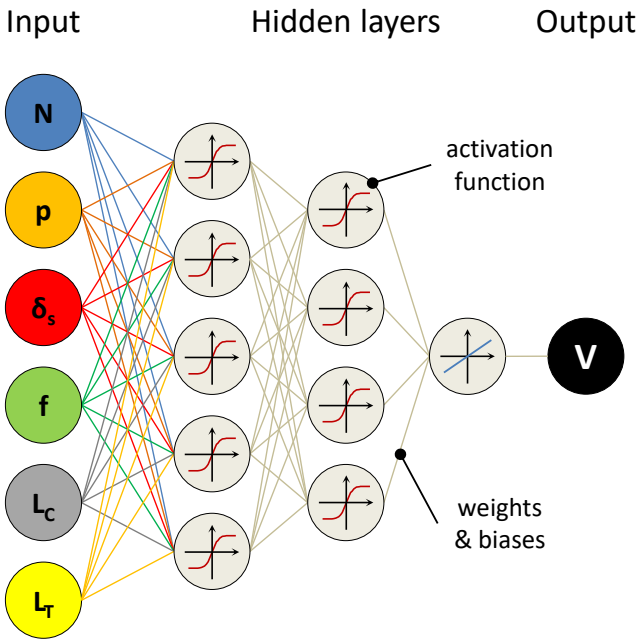

Fig. 4. Description of the artificial neural network used in the current study with six input loading parameters and one output parameter which is the wear volume.

After identifying the architecture of the ANN, a parametric study is done to choose the number of epochs and the learning rate, such that the number of epochs is varied from 10 to $2x10^4$ while the learning rate is fixed at a relatively low value that is equal to 0.00001. Then, the learning rate is varied from 0.1 to 10^{-6} while fixing the number of epochs at 10000. Subsequently, the percentage error (%E) between the experimental and the ANN predicted wear volume (Eq. 1) is estimated for each condition. As the choice of data is selected randomly during the training process to optimize the

performance of the ANN, %E will vary at each simulation. To estimate the variation of this error, the simulation is run 10 times at each imposed conditions of hyper parameters allowing the estimation of an average value and a standard deviation of %E.

$$E\% = \frac{100}{\frac{1}{n}\sum_{i=0}^{i=n} V_{exp,i}} \times \sqrt{\frac{\sum_{i=0}^{i=n} \left(V_{exp,i} - V_{pred,i}\right)^2}{n}} \quad \text{with } n = 150 \text{ experiments} \tag{1}$$

Fig. 5a shows that the %E decreases by increasing the number of epochs from 10 to 1000, following this it stabilizes at 25% when the number of epochs exceeds 1000. On the other hand, the %E is relatively low and stable around 25% when the learning rate is smaller than 10^{-4} (Fig. 5b), then it increases and becomes less stable when the learning rate exceeds 10^{-4}. Hence, in order to guarantee a stable and relatively low relative error less than 25% along with a relatively fast training time, the number of epochs and the learning rate in this study will be fixed at 10000 and 0.00001 respectively.

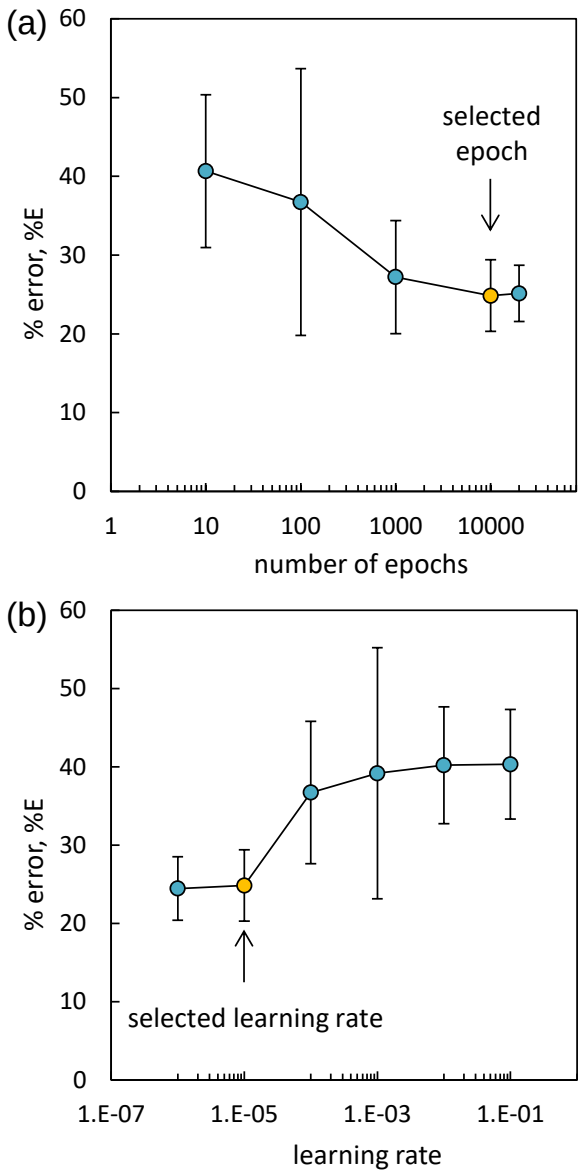

Fig. 5: Evolution of the percentage error (%E, Eq. 1) by varying the: (a) number of epochs from 10 to $2x10^4$ while fixing the learning rate at 0.00001; (b) learning rate from 0.1 to 10^{-6} while fixing the number of epochs at 10000 (in this parametric study, 70% of data is used for training, 10% for validation and 20% for testing procedure).

3.2 Results of ANN

Fig. 6 compares the evolution of the wear kinetics predicted by ANN to the trends obtained experimentally for each loading parameter.

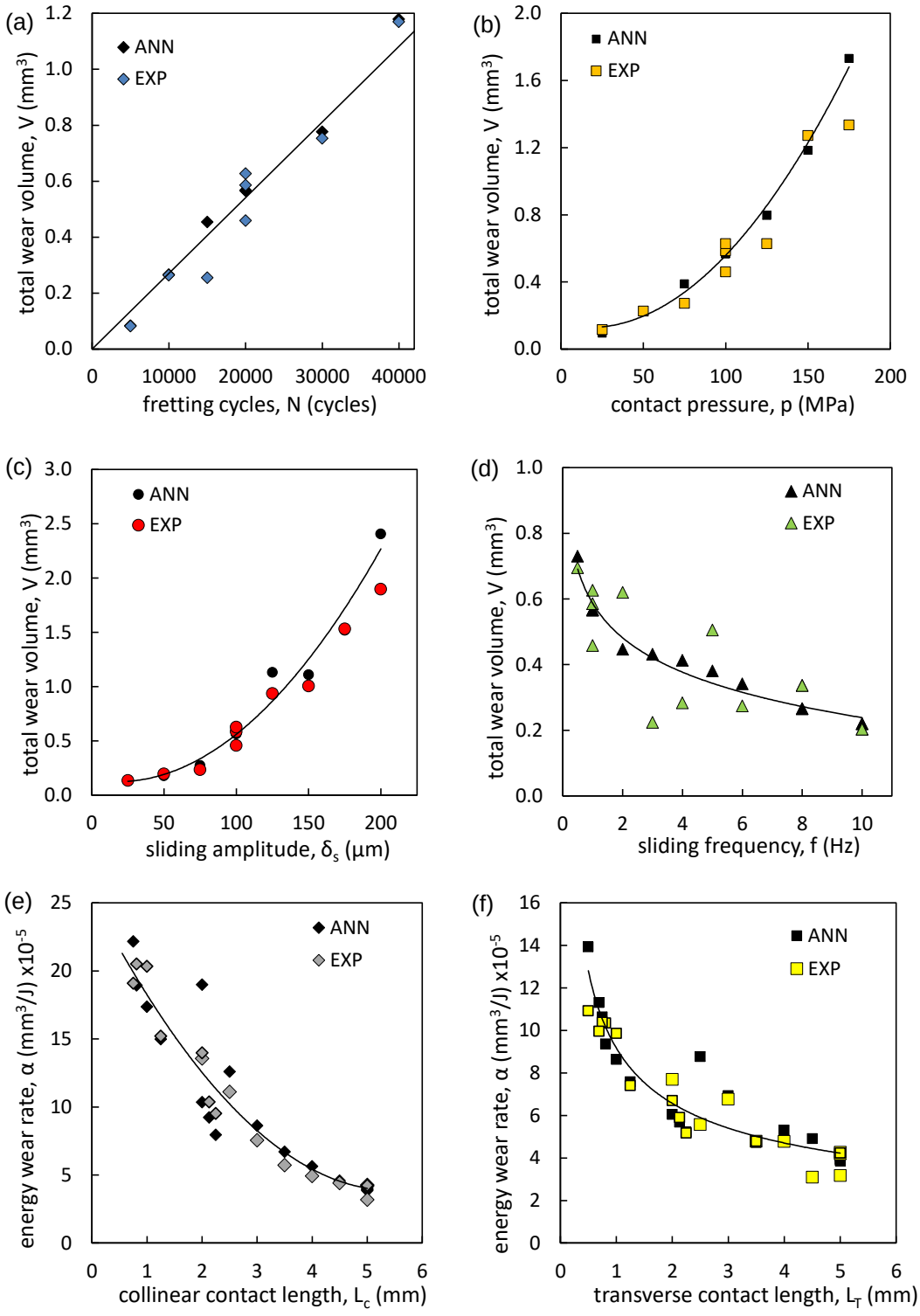

Fig. 6. Comparison between experimental and ANN evolution of wear kinetics as a function of loading parameters: (a) number of fretting cycles; (b) contact pressure; (c) sliding amplitude; (d) sliding frequency; (e) collinear contact length L_C; and (c) transverse contact length L_T.

It is remarked that the ANN perfectly predicts not only the linear tendency detected by varying the number of fretting cycles but also the decreasing and increasing nonlinear evolutions observed at the other loading parameters. This reflects the learning capacity of ANN and its ability to capture the regressions of more complex systems where larger number of input parameters is introduced.

Fig. 7 shows the evolution of the wear volume predicted by ANN compared to that obtained experimentally. In addition to the good prediction of the training and validation datasets, ANN has a very good performance on the test data corresponding to 30 randomly selected experiments the trained network has never seen but was able to predict with high accuracy. This reflects the generalizing ability of ANN in forecasting complex conditions. Besides, the percentage error (%E) between the experimental and the ANN predicted results (Eq. 1) is less than 20% signifying the reliability of this model in predicting wear volume.

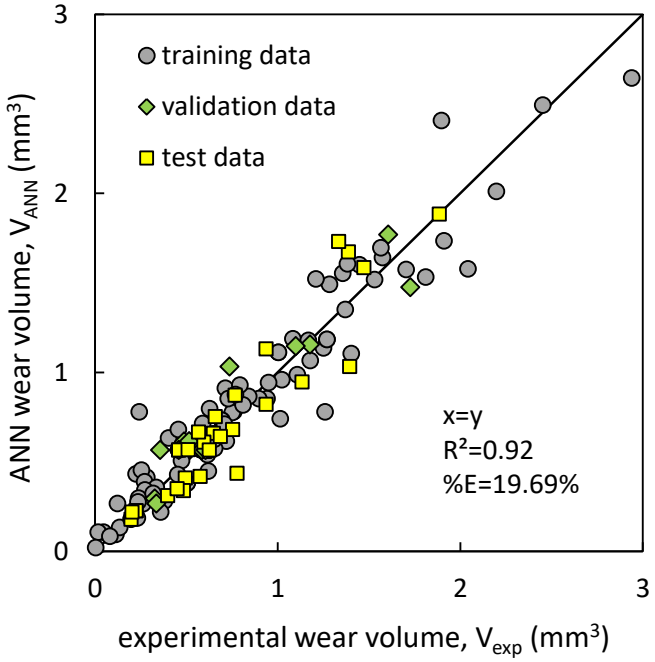

Fig. 7. Comparison between experimental wear volume and the wear volume predicted by ANN.

Fig. 8 pictures the evolution of the average error of the ANN predictions as a function of the percentage of data points used in training. Similarly to Section 3.1, as the choice of data is selected randomly during the training process, %E will vary at each simulation. To better assess the variation and the stability of this error, the simulation is run 10 times at each percentage of training data allowing the estimation of an average value and a standard deviation of %E. By increasing the percentage of training data from 10% to 70%, the error decreased from 60% to 25% respectively with a marked reduction in the standard deviation of %E. This reflects the necessity of having a sufficient quantity of training data to optimize the performance and the stability of the ANN predictions.

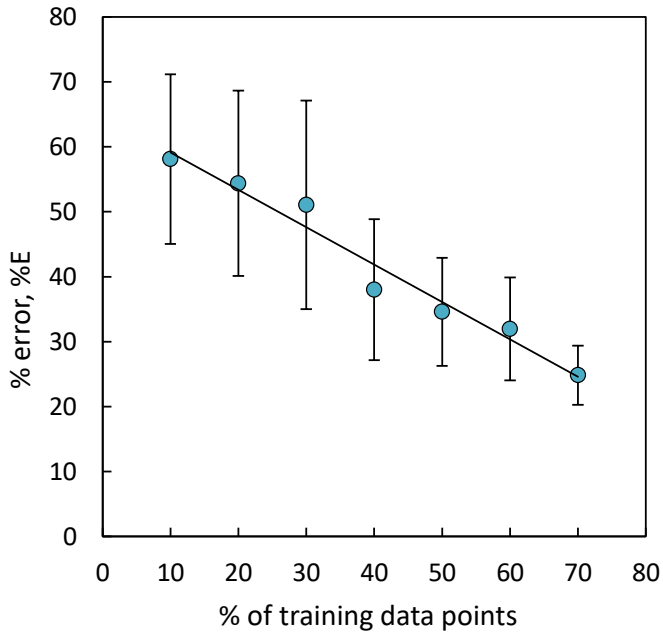

Fig. 8. Evolution of the ANN error %E (Eq. 1) as a function of the percentage of training data points.

4. Predicting wear volume using physical friction energy wear modeling

In this part, the wear volume prediction is predicted based on the energy wear law relating the wear volume (V) to the accumulated dissipated friction energy (∑Ed) at the interface through the energy wear rate α (such that V=αx∑Ed) [25]. Then, two cases will be assessed. In the first case, a plain friction energy wear model is investigated by considering a constant energy wear rate. In the second case, an extended friction energy wear model will be considered such that the energy wear rate will vary as a function of the loading parameters described in section 2.2.

4.1 Case 1: Plain friction energy wear model

In this case the energy wear rate is fixed at a constant value estimated by averaging the energy wear rates of a selected number of calibration data points “n” (Eq. 2).

$$V_{pred,\bar{\alpha}} = \bar{\alpha} \times \sum Ed \text{ where } \bar{\alpha} = \frac{1}{n}\sum_{i=0}^{i=n} \alpha_i \quad (2)$$

By averaging the energy wear rates of the entire data base with n=150 experiments to estimate “$\bar{\alpha}$”, bad predictions of the wear volume are obtained (Fig. 9) with %E=58.55%. This scattering suggests that the plain friction energy wear approach, being useful and easier to establish, is however not sufficiently elaborated to fully capture the effect of the studied loading parameters (i.e. contact pressure, frequency, sliding amplitude and contact size) on the fretting wear rates and consequently on the final fretting wear volumes.

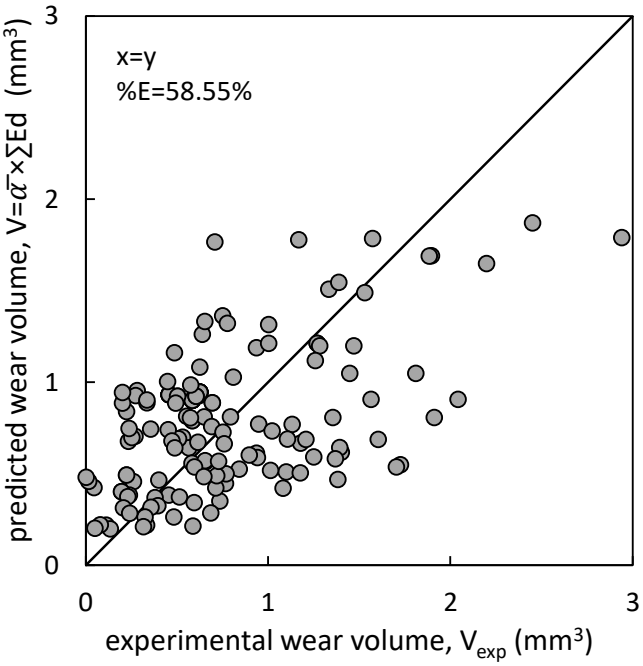

Fig. 9. Prediction of the experimental wear volume using the plain energy wear approach (Eq. 2) such that the energy wear rate is estimated by averaging the individual energy wear rates of all the data points (i.e. n=150 experiments).

4.2 Extended friction energy wear modeling

In order to ameliorate the wear volume prediction based on friction energy approach, this latter phenomenological modeling has been extended by integrating the effect of the loading parameters in the energy wear rate (α^*) through a factorial function of power law components with respect to the reference conditions indicated in section 2.2 [22].

$$V_{pred} = \alpha^* \times \sum Ed \text{ with } \alpha^* = \alpha_{ref} \times \prod \left(\frac{X}{X_{ref}}\right)^{n_X} \quad (3)$$

The contact loading parameter X can be substituted by L_{COC}, L_{TBT}, δ_s, p, N and f respectively where L_{COC} represents the minimum contact distance $L_{COC} = \min(L_C, L_T)$ permitting the oxygen diffusion to the interface. This latter affects the partition of the wear mechanisms (abrasion and adhesion) according to the contact oxygenation

concept (COC) which is fully detailed in a previous works [22]. On the other hand, L_{TBT} represents the length scale controlling the third body (i.e. wear particles) ejection process (i.e. Third Body Theory (TBT)) which corresponds to the collinear length scale (i.e. $L_{TBT} = L_C$) as detailed in [22]. In this research work, it was also shown that L_{TBT} and the sliding amplitude δ_s parameters can be combined by the ratio L_{TBT}/δ_s reflecting the synergic interaction between the collinear length scale and the fretting sliding amplitude regarding the debris ejection process. By merging these loading parameters, the energy wear rate can be extended as follows:

$$\alpha^* = \alpha_{ref} \times \left[\frac{N}{N_{ref}}\right]^{n_N} \times \left[\frac{L_{COC}}{L_{COC,ref}}\right]^{n_{COC}} \times \left[\frac{L_{TBT}/\delta_s}{L_{TBT,ref}/\delta_{s,ref}}\right]^{n_{TBT}} \times \left[\frac{p}{p_{ref}}\right]^{n_p} \times \left[\frac{f}{f_{ref}}\right]^{\eta_f} \quad (4)$$

The advantage of this energy wear model is that it requires small of quantity of data to be calibrated. This calibration is obtained by finding the unknown exponents (n_N, n_p, n_f, n_{TBT} and n_{COC}) which are obtained separately for each loading parameter by minimizing the standard deviation between the experimental total wear volume (V) and the predicted wear volume (V_{pred}) as detailed in [21]. Fig. 10 synthetizes the capacity of the given extended friction energy wear approach to predict the wear volume extension applying a wide range of fretting loadings and contact size configurations [22].

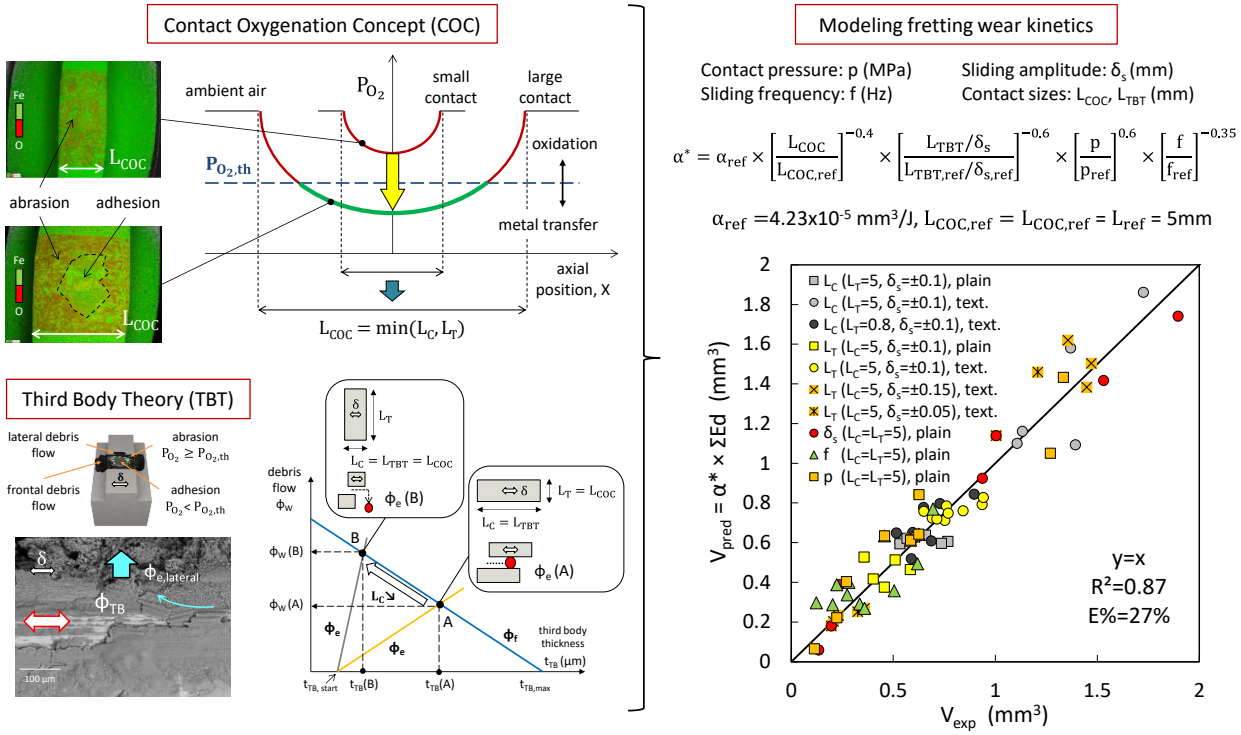

Fig. 10. Comparison between the experimental and the predicted wear volumes using the physical modeling (Eq. 4) such that N_{ref} = 20000 cycles, p_{ref}=100 MPa, f_{ref}= 1 Hz, $\delta_{s,ref}$= ±0.1 mm, $L_{COC,\ ref}$= $L_{TBT,\ ref}$= L_{ref}= 5 mm, α_{ref}= 4.23x10^{-5} mm^3/J, n_N= 0, n_p= 0.6, n_f= -0.35, n_{COC}= -0.4 and n_{TBT}= -0.6 [22].

5. Discussion

The objective of this section is to compare the efficiency of the ANN model versus the physics-based energy wear approach in predicting the wear volume when the quantity of training data points is varied. In the physics-based approaches, the number of the data points used in model calibration will be increased gradually as described in Fig. 11 such that the minimum number of data used is chosen from the extreme and medium tests for each loading condition. Following this, the number of data points and hence the percentage of calibration experiments will be progressively increased by nourishing the data base by additional internal data points as depicted in Fig. 11.

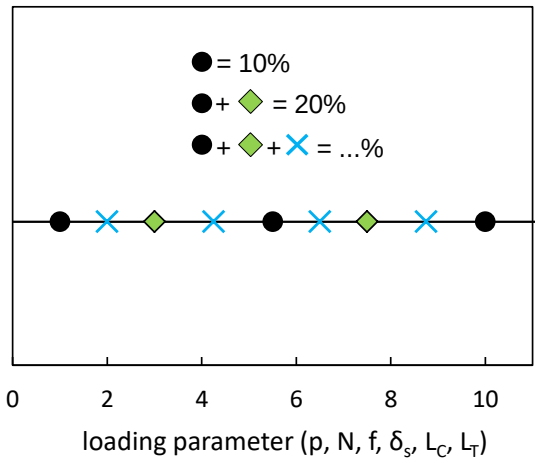

Fig. 11. Schematic description of the method used in selecting the data points used in energy wear model calibration.

Fig. 12 pictures the evolution of the average error of the ANN and friction energy wear model predictions as a function of the percentage of calibration data points. By considering first the plain friction energy wear model (Eq. 2) with constant energy wear rate, the error is relatively high and remains stable around 58% whatever the percentage of data points used in calibration.

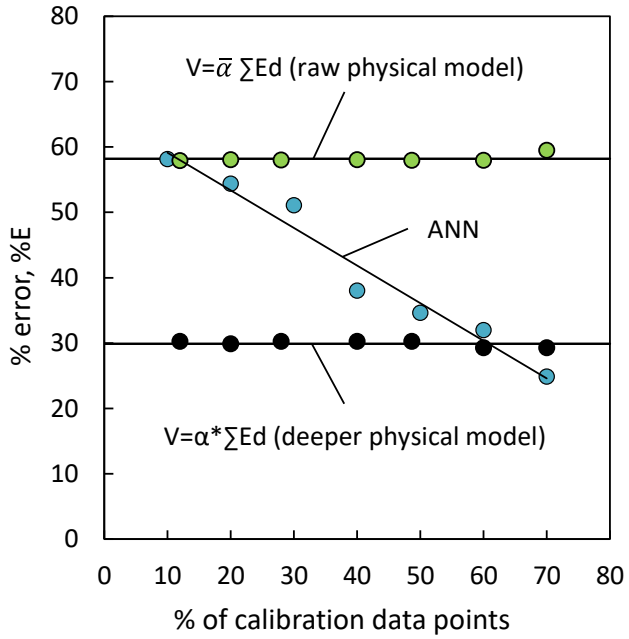

Fig. 12. Comparison between the prediction error of human regression model and ANN model (100% corresponds to 150 experiments).

On the other hand, using the extended friction energy wear approach ($V=\alpha^{*}\sum Ed$) and starting from at least three calibration experiments for each loading parameter, %E is around 30% which is nearly half the error obtained for ANN for the same quantity of calibration data. This error remains stable around 30% by increasing the number of training data of the model. This low and stable evolution of %E of the extended energy approach suggests that this latter is more representative of the physics of the studied fretting wear process as it considers both COC and TBT processes in its formulation. By contrast to the physical modeling which remains surprisingly stable whatever the percentage of calibration data points, the ANN displays a continuous decrease of %E. It is interesting to note that with only 10% of the training data, the ANN model performs the same as the plain friction energy model. However, this proportion must exceed 60% to equalize the performance of the extended friction energy wear approach. This suggests that ANN is equivalent to a raw physical model when a small quantity of data is available, yet it becomes equivalent to physics-based regression models only when a very large quantity of data is used for training the model (i.e. in the present analysis 60% of the data points). So, care should be taken when utilizing ANN especially that the model is less stable when a small number of experiments is available. This comparison underlines that the extended friction energy wear modeling, by capturing the physics of the surface damage mechanisms such as the contact oxygenation and the third body flows, is able to precisely predict the wear volume even when a restricted number of experiments is used for calibration. The deeper is the physical description, the better the predictions but also the lower the experimental cost to establish the parameters of the model.

Alternatively, if the physical model is not sufficiently elaborated, the ANN strategy appears more performant even with a restricted number of training data points. It should be noted that in this study the comparison between physics-based and ANN models is carried out by comparing their prediction efficiency when the percentage of data employed in the calibration (training) procedure is increased such that the maximum number of available experiments is 150. Hence, it would be interesting to check the effect of the absolute number of experiments in the stability of this analysis so that a precise limit can be defined between big data and small data which was not unfortunately investigated in this paper. Although 150 experiments seems a small database from a statistical point of view, it appears relatively large from a tribological standpoint. This is due to the fact that fretting tests are complex, expensive, and time consuming making it quite difficult to find larger datasets in literature. Additionally, fretting tests are reproducible as they only affect the extreme surface of the material; hence, they are less impacted by the microstructure and material defects that would generate higher dispersion in experimental results as the case of fretting-fatigue and cracking problems. Besides, the current neural network, aiming at fitting and predicting the linear or non-linear evolutions of the wear volume, is relatively simple compared to the complexity of larger neural networks as those involved in computer vision, image classification and speech recognition where thousands up to millions of training samples are required. These aspects together justify that the 150 experiments would be sufficient for the current study. Another aspect concerns the versatility of the models. For instance, the given extended friction energy wear modeling was developed for dry ambient temperature. Its extension to more complex ambient conditions like variable temperature or lubrication implies developing new physical models taking into account

for instance the occurrence of glaze layer [7] or tribofilms [26] respectively. This requires interesting but long and fastidious developments to elaborate adequate formalisms able to capture these various effects on the fretting wear rate fluctuations. A major interest of ANN is its capacity to be more easily transposed to predict such various ambient conditions. In the same vein, machine learning also appears potentially more efficient in modeling time-dependent processes as the evolution of friction coefficient as a function of time which can be predicted using recurrent neural networks.

6. Conclusion

In this work machine learning approach is applied to predict gross slip fretting wear response of low alloyed steel under different loading conditions. In particular, artificial neural network (ANN) is applied to predict wear volume. It appears that neural networks simulation succeeds in establishing the experimental linear and nonlinear dependencies of wear kinetics on the loading parameters but also predicts with sufficient accuracy the wear volume of significant portion of unseen test conditions. However, when compared to extended physical model, ANN requires large quantity of data points and becomes unreliable when small data base is utilized. However, it remains more performant than less extended physical models and in the presence of wider range of loading parameters as lubrication, contact temperature, etc. The given work also underlines the necessity to consider a significant quantity of experimental data to train the model. Current investigations are currently undertaken to establish the cost/result balance of such ANN strategy (i.e. number of experimental data required for the training process versus scattering of the prediction), but also to establish the potential gain versus more physical

wear modeling involving for instance the third body theory and/or the contact oxygenation concept [22,27].

Acknowledgements

This research did not receive any specific grant from funding agencies in the public, commercial, or not-for-profit sectors.

Reference

[1] P.L. Hurricks, The mechanism of fretting-A review, Wear. 15 (1970) 389–409. doi:10.1016/0043-1648(70)90235-8.
[2] O. Vingsbo, S. Soderberg, On fretting maps, Wear. 126 (1988) 131–147. doi:10.1016/0043-1648(88)90134-2.
[3] H. Proudhon, J.Y. Buffière, S. Fouvry, Three-dimensional study of a fretting crack using synchrotron X-ray micro-tomography, Eng. Fract. Mech. 74 (2007) 782–793. doi:10.1016/j.engfracmech.2006.06.019.
[4] M. Godet, The third-body approach: A mechanical view of wear, Wear. 100 (1984) 437–452. doi:10.1016/0043-1648(84)90025-5.
[5] J.M. Dobromirski, Variables of fretting process : Are there 50 of them?, Stand. Frett. Fatigue Test Methods Equipment. ASTM. (1992) 60–66.
[6] E.K. Hayes, P.H. Shipway, Effect of test conditions on the temperature at which a protective debris bed is formed in fretting of a high strength steel, Wear. 376–377 (2017) 1460–1466. doi:10.1016/j.wear.2017.01.057.
[7] A. Dreano, S. Fouvry, G. Guillonneau, Understanding and formalization of the fretting-wear behavior of a cobalt-based alloy at high temperature, Wear. 452–453 (2020) 203297. doi:10.1016/j.wear.2020.203297.
[8] S. Fouvry, P. Arnaud, A. Mignot, P. Neubauer, Contact size, frequency and cyclic normal force effects on Ti–6Al–4V fretting wear processes: An approach combining friction power and contact oxygenation, Tribol. Int. 113 (2017) 460–473. doi:10.1016/j.triboint.2016.12.049.
[9] A.R. Warmuth, S.R. Pearson, P.H. Shipway, W. Sun, The effect of contact geometry on fretting wear rates and mechanisms for a high strengthsteel, Wear. 301 (2013) 491–500. doi:10.1016/j.wear.2013.01.018.
[10] A.M. Kirk, W. Sun, C.J. Bennett, P.H. Shipway, Interaction of displacement amplitude and frequency effects in fretting wear of a high strength steel: Impact on debris bed formation and subsurface damage, Wear. 482–483 (2021) 203981. doi:10.1016/j.wear.2021.203981.
[11] T. Zhu, P.H. Shipway, Contact size and debris ejection in fretting: The inappropriate use of Archard-type analysis of wear data and the development of alternative wear equations for commonly employed non-conforming specimen pair geometries, Wear. 474–475 (2021) 203710. doi:10.1016/j.wear.2021.203710.
[12] M.B. Gorji, A. de Pannemaecker, S. Spevack, Machine learning predicts fretting and fatigue key mechanical properties, Int. J. Mech. Sci. 215 (2022) 106949. doi:10.1016/j.ijmecsci.2021.106949.
[13] S.P. Jones, R. Jansen, R.L. Fusaro, Preliminary investigation of neural network techniques to predict tribological properties, Tribol. Trans. 40 (1997) 312–320. doi:10.1080/10402009708983660.
[14] K. Velten, R. Reinicke, K. Friedrich, Wear volume prediction with artificial neural networks, Tribol. Int. 33 (2000) 731–736. doi:10.1016/S0301-679X(00)00115-8.
[15] R. Ramesh, R. Gnanamoorthy, Artificial neural network prediction of fretting wear behavior of structural steel, en 24 against bearing steel, en 31, J. Mater. Eng. Perform. 16 (2007) 703–709. doi:10.1007/s11665-007-9100-9.
[16] F. Aydin, R. Durgut, Estimation of wear performance of AZ91 alloy under dry sliding conditions using machine learning methods, Trans. Nonferrous Met. Soc. China (English Ed. 31 (2021) 125–137. doi:10.1016/S1003-6326(20)65482-6.
[17] L. Haviez, R. Toscano, M. El Youssef, S. Fouvry, G. Yantio, G. Moreau, Semi-physical neural network model for fretting wear estimation, J. Intell. Fuzzy Syst. 28 (2015) 1745–1753. doi:10.3233/IFS-141461.
[18] S. Anand Kumar, S. Ganesh Sundara Raman, T.S.N. Sankara Narayanan, R. Gnanamoorthy, Prediction of fretting wear behavior of surface mechanical attrition treated Ti-6Al-4V using artificial neural network, Mater. Des. 49 (2013) 992–999. doi:10.1016/j.matdes.2013.02.076.
[19] D. Nowell, P.W. Nowell, A machine learning approach to the prediction of fretting fatigue life, Tribol. Int. 141 (2020) 105913. doi:10.1016/j.triboint.2019.105913.
[20] T. Kolodziejczyk, R. Toscano, S. Fouvry, G. Morales-Espejel, Artificial intelligence as efficient technique for ball bearing fretting wear damage prediction, Wear. 268 (2010) 309–315. doi:10.1016/j.wear.2009.08.016.

[21] S. Baydoun, S. Fouvry, S. Descartes, P. Arnaud, Fretting wear rate evolution of a flat-on-flat low alloyed steel contact: A weighted friction energy formulation, Wear. 426–427 (2019) 676–693. doi:10.1016/j.wear.2018.12.022.
[22] S. Baydoun, S. Fouvry, S. Descartes, Modeling contact size effect on fretting wear: A combined contact oxygenation - Third body approach, Wear. 488–489 (2021) 204168. doi:10.1016/j.wear.2021.204168.
[23] S. Baydoun, P. Arnaud, S. Fouvry, Explicit formulations of adhesive wear extension in fretting interfaces applying the contact oxygenation concept, Wear. 488–489 (2022) 204147. doi:10.1016/j.wear.2021.204147.
[24] S. Baydoun, P. Arnaud, S. Fouvry, Modelling adhesive wear extension in fretting interfaces: An advection-dispersion-reaction contact oxygenation approach, Tribol. Int. 151 (2020) 106490. doi:10.1016/j.triboint.2020.106490.
[25] S. Fouvry, P. Kapsa, An energy description of hard coating wear mechanisms, Surf. Coatings Technol. 138 (2001) 141–148. doi:10.1016/S0257-8972(00)01161-0.
[26] J. He, J. Peng, Y. Ren, Z. Cai, J. Liu, M. Zhu, Study on improving fretting wear properties of AISI 4135 steel via diverse surface modifications under grease lubrication, Wear. 490–491 (2022) 204210. doi:10.1016/j.wear.2021.204210.
[27] P. Arnaud, S. Baydoun, S. Fouvry, Modeling adhesive and abrasive wear phenomena in fretting interfaces: A multiphysics approach coupling friction energy, third body and contact oxygenation concepts, Tribol. Int. 161 (2021) 107077. doi:10.1016/j.triboint.2021.107077.